

Fusion hindrance for Ca + Ca systems: Influence of neutron excess

C. L. Jiang,¹ A. M. Stefanini,² H. Esbensen,¹ K. E. Rehm,¹ L. Corradi,² E. Fioretto,² P. Mason,³ G. Montagnoli,³ F. Scarlassara,³ R. Silvestri,² P. P. Singh,² S. Szilner,⁴ X. D. Tang,⁵ and C. A. Ur³

¹Physics Division, Argonne National Laboratory, Argonne, Illinois 60439, USA

²INFN, Laboratori Nazionali di Legnaro, I-35020 Legnaro (Padova), Italy

³Dipartimento di Fisica, Università di Padova, and INFN, Sezione di Padova, I-67037 Padova, Italy

⁴Ruder Boskovic Institute, HR-10002 Zagreb, Croatia

⁵Department of Physics, University of Notre Dame, Notre Dame, Indiana 46556, USA

(Received 20 September 2010; published 19 October 2010)

The measurement of the excitation function for fusion evaporation reactions in the system $^{40}\text{Ca} + ^{48}\text{Ca}$ ($Q = 4.56$ MeV) has been extended downward by two orders of magnitude with respect to previous cross section data. A first indication of an S -factor maximum in a system with a positive Q value has been observed. In addition a correlation between fusion hindrance and neutron excess $N - Z$ has been found for the Ca + Ca, Ni + Ni, and Ca + Zr systems.

DOI: [10.1103/PhysRevC.82.041601](https://doi.org/10.1103/PhysRevC.82.041601)

PACS number(s): 25.60.Pj, 26.50.+x, 25.70.-z, 26.30.-k

Fusion hindrance at extreme low energies—a falloff of the fusion cross sections, which is steeper than predicted by standard coupled-channels (CC) calculations—is a well established phenomenon in reactions between medium-mass nuclei [1]. Experimentally the falloff has been studied either by analyzing the logarithmic derivative of the fusion cross section ($L(E) = d[\ln(\sigma E)/dE]$) or by introducing the so-called S factor [$S(E) = \sigma E \exp(2\pi\eta)$], which partially eliminates the strong energy dependence of the fusion cross section at low energies. In the S -factor representation, a maximum in $S(E)$ appears for all systems with negative Q values. This behavior can be understood from the definition of $S(E)$: since $\sigma(E)$ has to be zero for energies $E \leq -Q$, the S factor will also be zero. While many studies have shown that fusion hindrance seems to be common to all heavy-ion fusion reactions, even for systems with positive Q values [2–6], a detailed understanding of fusion hindrance in systems with a positive Q value is still missing. Answers to these questions are not only essential for a better insight into the fusion mechanism, but they are also relevant to nuclear astrophysics. Since the critical energy regions for carbon and oxygen burning are still unattainable to cross section measurement in the laboratory, extrapolations to lower energies must be used, which are strongly influenced by the fusion hindrance behavior.

In three earlier experiments, fusion excitation functions for the systems $^{28}\text{Si} + ^{30}\text{Si}$ ($Q = 14.3$ MeV) [7], $^{36}\text{S} + ^{48}\text{Ca}$ ($Q = 7.55$ MeV) [8], and $^{27}\text{Al} + ^{45}\text{Sc}$ ($Q = 9.63$ MeV) [9] were measured down to ~ 40 μb , 600 nb, and 300 nb, respectively. Indications of fusion hindrance have been observed in all of these systems since the excitation functions drop faster than predicted by the standard CC calculations. However, no evidence of an S factor maximum has been observed in the energy ranges covered by the experiments. On the other hand, in a measurement of the system $^{48}\text{Ca} + ^{48}\text{Ca}$ ($Q = -2.99$ MeV) it was observed that the experimental $S(E)$ and $L(E)$ curves at low energies are nearly identical to the result obtained for the reaction $^{36}\text{S} + ^{48}\text{Ca}$ ($Q = 7.55$ MeV). No evidence of an S -factor maximum was observed at energies,

which were 6 MeV below the energy E_s^{emp} , expected for an S -factor maximum in Ref. [10].

In order to investigate this question in more detail we have remeasured the fusion excitation function for the system $^{40}\text{Ca} + ^{48}\text{Ca}$ ($Q = 4.56$ MeV), which had previously been measured down to cross sections of about 500 μb [11,12], well above the energy region where fusion hindrance plays a role.

The experiment was performed at the XTU Tandem accelerator of Laboratori Nazionali di Legnaro, Italy. A ^{40}Ca beam of 5–10 pA bombarded a CaF_2 target (thickness 50 $\mu\text{g}/\text{cm}^2$, evaporated on a 20 $\mu\text{g}/\text{cm}^2$ carbon backing). The isotopic abundance of ^{48}Ca was 96.78%. The evaporation residues were detected with the electrostatic separator in its upgraded configuration. The detector system consists of two microchannel plate detectors, one ionization chamber, and a silicon surface-barrier detector. Details of the experimental setup, and the analysis have been described in Refs. [5,8,10,13].

A clear signature of the evaporation residues was obtained in this experiment. Spectra of ΔE versus E_{tot} at the two lowest energies are shown in Fig. 1(a). These spectra are gated by several time-of-flight windows. Solid red and black circles are results at the two lowest energies. Also shown by the open blue circles are fusion events obtained in a run at $E_{\text{lab}} = 89.2$ MeV. The solid line represents the acceptance area for evaporation residues.

The angular distribution of evaporation residues measured with the electrostatic separator at $E_{\text{lab}} = 107.7$ MeV is presented in Fig. 1(b). The distribution can be well described by two Gaussians, as shown by the dashed and solid lines.

Experimental excitation functions for the system $^{40}\text{Ca} + ^{48}\text{Ca}$ are plotted in Fig. 2(a). The red circles are from this measurement, while two previous experiments for the same system by Trotta *et al.* [11] and Aljuwair *et al.* [12] are shown by green upward-triangles and black downward-triangles, respectively. The uncertainties for the present data are statistical only. The cross sections at the two lowest energies were obtained from two and nine counts, respectively. The uncertainty of the absolute cross sections is estimated to be about $\pm 7\%$.

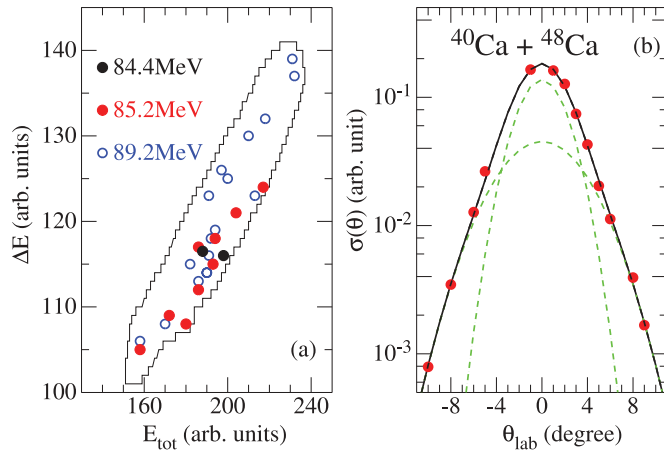


FIG. 1. (Color online) (a) Fusion events in a spectrum of ΔE versus E_{tot} measured at the two lowest energies in this experiment together with data obtained at $E_{\text{lab}} = 89.2$ MeV. (b) Angular distribution of evaporation residues measured at $E_{\text{lab}} = 107.7$ MeV. The uncertainties in cross sections are smaller than the sizes of the circles. The distribution can be well described by two Gaussians as shown by the dashed and solid lines.

Our results agree well with Aljuwair's data [12], but are much lower than the data by Trotta *et al.* [11]. The reason for this difference is unclear. The transmission of the electrostatic separator was measured in the present experiment and the absolute values of the present cross sections were checked again in two subsequent measurements. It should be mentioned that in the recent measurement of $^{48}\text{Ca} + ^{48}\text{Ca}$ [10], the absolute cross sections obtained are also smaller by 20% when compared to the results obtained previously by Trotta *et al.* [11]. Because the signature of fusion hindrance is sensitive to relative cross sections, the analysis presented below is independent of the absolute normalization.

As seen from Fig. 2(a) the present experiment has extended the cross section measurement by more than two orders

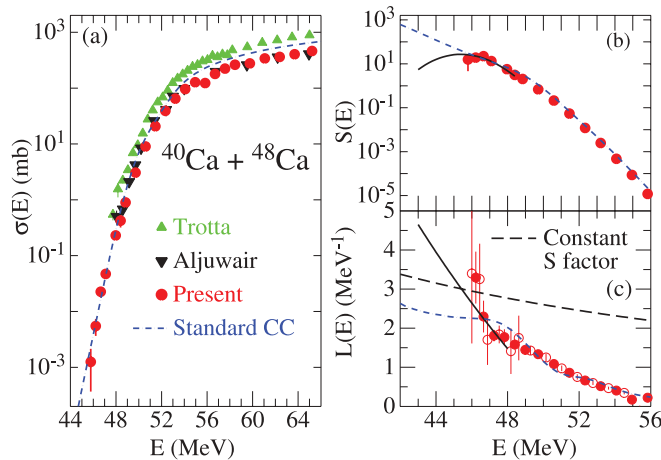


FIG. 2. (Color online) (a) Excitation functions of $^{40}\text{Ca} + ^{48}\text{Ca}$ measured in three different experiments. (b), (c) The corresponding $S(E)$ and $L(E)$ curves from the present measurement. The open and closed circles for the logarithmic derivative are obtained by using two or three adjacent data points, respectively.

of magnitude, down to $\sim 1 \mu\text{b}$, where fusion hindrance is expected to appear. The $S(E)$ factor and the logarithmic derivative $L(E)$ from the present measurement are shown in Fig. 2(b) and 2(c), respectively. The dashed curve in Fig. 2(c) is the constant S -factor function, $L_{cs}(E) = \pi\eta/E$. It can be seen that the measured $L(E)$ crosses the constant S -factor curve at the lowest energies. The crossing point, at energy E_s , corresponds to the S -factor maximum which can be seen in Fig. 2(b). It is clear that more data points at even lower energies are desirable.

The solid black curve in Fig. 2(c) is a fit to the low energy part of the experimental derivative $L(E)$ using the function [6]

$$L(E) = A_0 + B_0/E^{3/2}. \quad (1)$$

The solid black curve in Fig. 2(b) is the corresponding $S(E)$ obtained from [6]:

$$\sigma(E) = \sigma_s \frac{E_s}{E} e^{[A_0(E-E_s) - B_0 \frac{1}{E_s^{1/2}(1/2)}] [\frac{E_s}{E}]^{1/2} - 1]}. \quad (2)$$

The parameters A_0 , B_0 , E_s , and σ_s obtained are -16.2 MeV^{-1} , $5887 \text{ MeV}^{1/2}$, 45.4 MeV , and $6.8 \mu\text{b}$, respectively, where σ_s is the cross section at the energy E_s of the S -factor maximum. The dash-dotted curves in Fig. 2 are from standard CC calculations.

In Fig. 3(a) and 3(b) $S(E)$ factors and logarithmic derivatives $L(E)$ are compared for the three different systems: $^{40}\text{Ca} + ^{48}\text{Ca}$, $^{40}\text{Ca} + ^{40}\text{Ca}$, and $^{48}\text{Ca} + ^{48}\text{Ca}$. The $S(E)$ curves have been normalized to overlap at the higher energies. It can be seen that the behavior of $S(E)$ for these three systems at the lowest energies is very different. This points to a possible nuclear structure effect, which will be discussed in the following.

From Fig. 3(b), it can be seen, the $L(E)$ for the systems $^{40}\text{Ca} + ^{48}\text{Ca}$ and $^{48}\text{Ca} + ^{48}\text{Ca}$ experience a smaller slope in $L(E)$ at the lowest energies, in agreement with the CC calculations. Only the system $^{40}\text{Ca} + ^{48}\text{Ca}$ has been measured to low enough energies, so that the steep rise and a subsequent

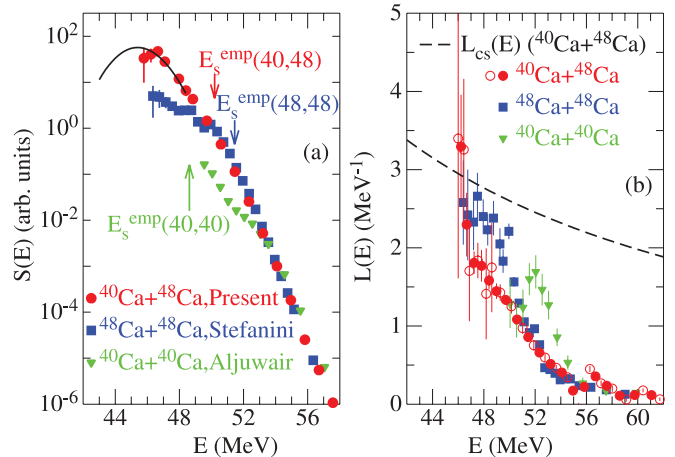


FIG. 3. (Color online) Comparison of $S(E)$ factors and logarithmic derivatives $L(E)$ for the three systems, $^{40}\text{Ca} + ^{48}\text{Ca}$, $^{40}\text{Ca} + ^{40}\text{Ca}$, and $^{48}\text{Ca} + ^{48}\text{Ca}$. The arrows in (a) give the energy locations of S -factor maxima for the three systems predicted by systematics. The dashed line in (b), representing the constant S -factor curve $L_{cs}(E)$, is for $^{40}\text{Ca} + ^{48}\text{Ca}$.

crossing of $L(E)$ with the constant S -factor curve $L_{cs}(E)$ has been observed. For the system $^{48}\text{Ca} + ^{48}\text{Ca}$ no S -factor maximum yet has been observed. The system $^{40}\text{Ca} + ^{40}\text{Ca}$ was studied before fusion hindrance had been discovered and the measurements stopped at cross sections of about 0.2 mb. Thus, no S -factor maximum has been seen for this system.

From systematics, the S -factor maxima are expected to occur at energies, E_s^{emp} , which are shown by arrows in Fig. 3(a). They are calculated from the formula [6]

$$E_s^{\text{emp}} = [0.495\zeta/L_s^{\text{emp}}(\zeta)]^{2/3} \quad (\text{MeV}), \quad (3)$$

with $L_s^{\text{emp}} = 2.33 + 580/\zeta$ and $\zeta = Z_1 Z_2 \sqrt{\mu}$, where μ is the reduced mass of the colliding nuclei.

Equation (3) was obtained from systems, whose colliding partners are mainly closed shell nuclei. For other systems, the values of E_s^{emp} have to be considered as upper limits of E_s . As already observed in the Ni + Ni [1] and Ca + Zr [14] systems, nuclear structure effects such as the neutron excess $N - Z$ can lead to deviations of the energy E_s of the S -factor maximum from the corresponding empirical values E_s^{emp} . The relations between the difference $E_s - E_s^{\text{emp}}$ and the neutron excess $N - Z$ for systems, where a large chain of isotopic combinations has been measured, is compared in Fig. 4. The solid line gives the empirical energy E_s^{emp} from Eq. (3) (Ref. [6]). Most symbols are obtained from the extrapolations of the logarithmic derivatives [1,14]. For the system $^{40}\text{Ca} + ^{40}\text{Ca}$, the cross section measurements do not extend far enough to obtain a reliable prediction. The value for this system predicted from the systematics is $E_s = 48$ MeV. A long vertical symbol is thus shown for $^{40}\text{Ca} + ^{40}\text{Ca}$. The data in Fig. 4 point to a correlation between E_s and the value of $N - Z$. As shown, the largest deviations from the empirical energies E_s^{emp} are observed for the systems with the largest neutron excess $N - Z$.

The similarity is even more noticeable in a direct comparison of the fusion excitation functions for the Ca + Ca and Ca + Zr systems (see Fig. 5). The low-energy enhancement of the $^{40}\text{Ca} + ^{48}\text{Ca}$ fusion cross sections is very similar to the one observed in the system $^{40}\text{Ca} + ^{96}\text{Zr}$. In these two sets of systems, the strongest influence of transfer reactions on fusion is expected for $^{40}\text{Ca} + ^{48}\text{Ca}$ and $^{40}\text{Ca} + ^{96}\text{Zr}$ which

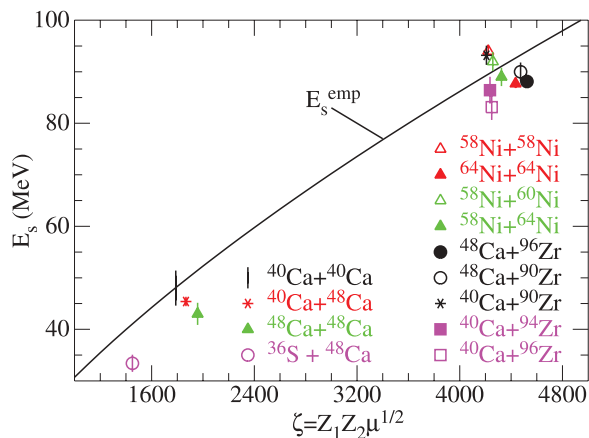


FIG. 4. (Color online) Plot of E_s versus ζ for the systems of Ca + Ca, Ni + Ni, and Ca + Zr.

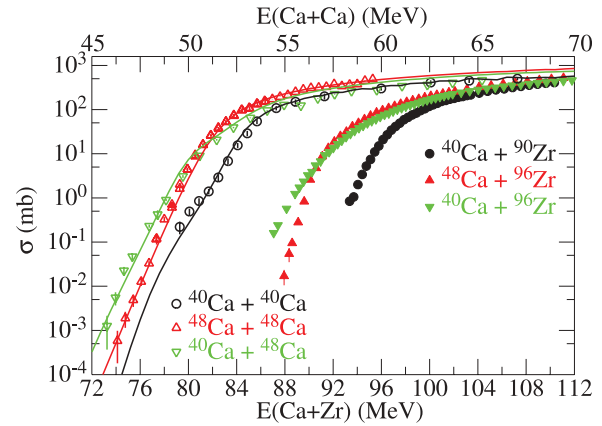


FIG. 5. (Color online) Comparison of excitation functions for the systems of Ca + Ca [10,12] and Ca + Zr [15,16].

might explain the peculiar ordering of the excitation functions at low energies in Fig. 5. In order to explain the $^{40}\text{Ca} + ^{48}\text{Ca}$ fusion data of Ref. [12], the influence of transfer on fusion has been already investigated previously [17,18]. It was especially pointed out in Ref. [17] that, a strong pair-transfer channel with a positive Q value was necessary to be included into the CC calculations. The elastic scattering data are also consistent with the existence of a such strong coupling [19].

Fusion hindrance has been studied using several theoretical approaches. Among them, two models have been quite successful. In Ref. [20] a repulsive potential was introduced which is related to the saturation property of nuclear matter. Many experimental results, mainly involving medium-mass nuclei, have been reproduced by this model. In a different model [21], the approach phase of the collision has been studied in detail and a two-step, adiabatic model was developed which is also in good agreement with the experimental data.

The data from the present experiment have been analyzed within the repulsive-core model of Ref. [20]. The M3Y+repulsion potentials are generated using the known densities of ^{40}Ca and ^{48}Ca , obtained from electron scattering experiments. The parameters of the repulsive interaction are $a_r = 0.41$ fm and $V_r = 471.4$ MeV, respectively, giving a nuclear incompressibility, $K = 234$ MeV. These potentials were used for a description of the fusion data $^{40}\text{Ca} + ^{40}\text{Ca}$ and $^{48}\text{Ca} + ^{48}\text{Ca}$. There are nine inelastic excitation channels in the basic calculations including all one-phonon excitations of the 2^+ , 3^- , and 5^- states plus the two-phonon excitation of the 2^+ state.

As mentioned above, in order to explain the fusion of $^{40}\text{Ca} + ^{48}\text{Ca}$ it is necessary to include couplings to transfer channels, in particular to those with positive Q values. The coupled-channels treatment of transfer is in general a complex problem because there are many channels that have to be considered. However, we may follow the simple method that was developed in Ref. [17]. In that approach the one-proton transfer channels with positive Q values were included, where as the one-neutron transfer channels can be ignored since the Q values are negative. The different one-proton transfer channels were combined into one effective transfer channel as described in Ref. [17]. A successive two-proton transfer was also considered by applying the same form factor that describes

the one-step proton transfer. The Q values for the direct two-proton and two-neutron transfers are both positive (see Table IV of Ref. [17]). These two transfers were simulated in the calculations by one effective pair-transfer channel with an effective Q value of 1 MeV. The pair-transfer was described by the macroscopic form factor proposed by Dasso and Pollarolo [22]. The coupling strength of the pair-transfer was adjusted to provide an optimum fit to the fusion data.

Overall, the coupled-channels calculations shown in Fig. 5 for the three fusion reactions of Ca + Ca provide a good description of the experimental data. Details of the calculations will be published separately [23].

In summary, a first indication of an S -factor maximum in a system with a positive Q value has been observed. If confirmed in other systems with positive Q values, this effect will play an important role in nuclear astrophysics

where fusion reactions occur at very low energies which are presently inaccessible to laboratory studies and thus require extrapolations. In addition an interesting correlation between fusion hindrance and neutron excess $N - Z$ has been found.

We want to thank the staff of the XTU Tandem for providing the excellent ^{40}Ca beams. The help of Mr. Loriggiola in preparing the ^{48}Ca targets is gratefully acknowledged. We also thank B. B. Back and R. V. F. Janssens for valuable discussions. This work was partially supported by the US Department of Energy, Office of Nuclear Physics under Contract No. DE-AC02-06CH11357, by the European Commission within the 6th Framework Programme through I3-EURONS (Contract No. RII3-CT-2004-506065), the Croatian MZOS 0098-1191005-2890 grant, and by the NSF under Contract No. PHY07-58100.

-
- [1] C. L. Jiang *et al.*, *Phys. Rev. Lett.* **89**, 052701 (2002); **93**, 012701 (2004); *Phys. Rev. C* **71**, 044613 (2005); *Phys. Lett. B* **640**, 18 (2006).
- [2] C. L. Jiang, H. Esbensen, B. B. Back, R. V. F. Janssens, and K. E. Rehm, *Phys. Rev. C* **69**, 014604 (2004); C. L. Jiang, B. B. Back, H. Esbensen, R. V. F. Janssens, and K. E. Rehm, *ibid.* **73**, 014613 (2006); C. L. Jiang, B. B. Back, R. V. F. Janssens, and K. E. Rehm, *ibid.* **75**, 057604 (2007).
- [3] M. Dasgupta *et al.*, *Phys. Rev. Lett.* **99**, 192701 (2007).
- [4] M. Trotta *et al.*, *Nucl. Phys. A* **787**, 134c (2007).
- [5] A. M. Stefanini *et al.*, *Phys. Rev. C* **82**, 014614 (2010).
- [6] C. L. Jiang, K. E. Rehm, B. B. Back, and R. V. F. Janssens, *Phys. Rev. C* **75**, 015803 (2007); **79**, 044601 (2009).
- [7] C. L. Jiang *et al.*, *Phys. Rev. C* **78**, 017601 (2008).
- [8] A. M. Stefanini *et al.*, *Phys. Rev. C* **78**, 044607 (2008).
- [9] C. L. Jiang *et al.*, *Phys. Rev. C* **81**, 024611 (2010).
- [10] A. M. Stefanini *et al.*, *Phys. Lett. B* **679**, 95 (2009).
- [11] M. Trotta *et al.*, *Phys. Rev. C* **65**, 011601(R) (2001).
- [12] H. A. Aljuwair *et al.*, *Phys. Rev. C* **30**, 1223 (1984).
- [13] A. M. Stefanini *et al.*, *Phys. Rev. C* **81**, 037601 (2010).
- [14] H. Esbensen and C. L. Jiang, *Phys. Rev. C* **79**, 064619 (2009).
- [15] H. Timmers *et al.*, *Nucl. Phys. A* **633**, 421 (1998).
- [16] A. M. Stefanini *et al.*, *Phys. Rev. C* **73**, 034606 (2006).
- [17] H. Esbensen, S. H. Fricke, and S. Landowne, *Phys. Rev. C* **40**, 2046 (1989).
- [18] V. I. Zagrebaev, *Phys. Rev. C* **67**, 061601(R) (2003).
- [19] R. J. Tighe *et al.*, *Phys. Rev. C* **42**, R1200 (1990).
- [20] Ş. Mişicu and H. Esbensen, *Phys. Rev. Lett.* **96**, 112701 (2006).
- [21] T. Ichikawa, K. Hagino, and A. Iwamoto, *Phys. Rev. C* **75**, 064612 (2007).
- [22] C. H. Dasso and G. Pollarolo, *Phys. Lett. B* **155**, 223 (1985).
- [23] H. Esbensen, C. L. Jiang, and A. M. Stefanini (submitted to *Phys. Rev. C*).